NUCL SCI TECH (2018) 29:146
https://doi.org/10.1007/s41365-018-0482-1

Product yields for the photofission of ^{232}Th, ^{234,238}U, ^{237}Np, and ^{239,240,242}Pu actinides at various incident photon energies

M. R. Pahlavani[1] · **P. Mehdipour**[1]

Received: 2 January 2018 / Revised: 15 May 2018 / Accepted: 4 June 2018 / Published online: 31 August 2018

Abstract Photofission fragments mass yield for ^{232}Th, ^{234,238}U, ^{237}Np, and ^{239,240,242}Pu isotopes are investigated. The calculations are done using a developed approach based on Gorodisskiy's phenomenological formalism. The Gorodisskiy's method is developed to be applied for the neutron-induced fission. Here we revised it for application to photofission. The effect of emitted neutron prior to fission on the fission fragment mass yields has also been studied. The peak-to-valley ratio is extracted for the ^{240}Pu isotope as a function of energy. Obtained results of the present formalism are compared with the available experimental data. Satisfactory agreement is achieved between the results of present approach and the experimental data.

Keywords Fission fragments · Fragment mass yield · Photofission · Neutron fission · Heavy nuclei · Peak-to-valley

1 Introduction

In spite of peaceful application in energy production, different features of various kinds of fission are not known yet. Photofission is one way to induce fission on actinides (U, Pu, Np, etc.). Although photofission was discovered more than fifty years ago [1], its theoretical modeling was produced with many challenges. Various theoretical approaches [2–7] have been presented to evaluate fragment mass yields for neutron(proton)-induced fission, but there is no comprehensive method to study photofission. The distribution of fragment mass yield plays a significant role in examining the validity of every theoretical method of fission. If the calculated fragment mass yields are well fitted with measured data, this means that the selected model is suitable to be applied for the fission process. In the statistical model of Wilkins [8, 9] and its developed version by Moreau [10], the probability of fission for neutron-induced fission is presented as follows:

$$P \sim \mathrm{e}^{(-E_{\mathrm{total}}/T)} = \mathrm{e}^{(-(E_{\mathrm{mac}}+E_{\mathrm{mic}})/T)}, \quad (1)$$

where P is the probability of fission and E_{total} includes all kinds of energies presented in the evaluation of compound nucleus from saddle to scission point. E_{mac} and E_{mic} are the macroscopic and microscopic energies, respectively. The relation between fission fragments mass yield and fragment mass number indicates that the probability appears in the Gaussian form. Therefore, the theoretical neutron-induced fission models are developed in the form of a multi-Gaussian shape and are formulated as a sum of several Gaussian-type function [11–13].

The old formalism presented by Wang Fu-cheng [5] was applicable for reproducing low-energy fission and contains five Gaussian terms. The formalism of Robert Mills [14], in which the dependence on energy was neglected, includes four Gaussian terms in the quadratic structure. The GEF computer code [15] is developed based on this method with various assumptions and many adjustable parameters. The complicated Langevin–Brownian method has been employed to study neutron-induced fission and lunched some success in recent years [16–21]. Recently, the Gorodisskiy phenomenological method [22] has been successful in reproducing the experimental data for

✉ M. R. Pahlavani
m.pahlavani@umz.ac.ir

[1] Department of Physics, Faculty of Basic Science, University of Mazandaran, P.O. Box 47415-416, Babolsar, Iran

neutron-induced fission of actinides. It is clear that the photofission process is similar to neutron-induced fission except in multi-polarity absorptions and time scale of the fission process. These absorptions happen in the beginning of the process; therefore, after formation of the compound nucleus, the fission process of the neutron-induced fission will become similar to photofission. According to the Bohr's hypothesis, the compound nucleus rapidly loses its total formation memory except conserved degrees of freedom. Therefore, the mode of decay of the compound nucleus does not depend on the way the compound nucleus is formed. Thus, for the same excited configuration of the compound nucleus, the photofission fragment mass yield is expected to be approximately similar to the neutron-induced fission. In the present study, we examined an extended version of the Gorodisskiy's method to generate the photofission fragment mass yield. The relative contributions of the symmetric and the asymmetric yields (Y_s and Y_a) of the Gorodisskiy's method and the variance of asymmetric fission (σ_a) are modified. The detail of modification is presented in the next section. The paper is constructed as follows: Theoretical model used to calculate the fission fragments mass distribution is presented in Sect. 2. In Sect. 3, theoretical results are compared with the experimental data for different excitation energies and different numbers of emitted neutron prior to fission for ^{232}Th, ^{234,238}U, ^{237}Np, and ^{239,240,242}Pu actinides. Finally, a short conclusion is presented in Sect. 4.

2 Description of theoretical model

Studies of fission fragments mass distribution of most fissioning nuclei indicate that the yield of fission fragments as a function of fragment mass number (A) is a Gaussian function with 4 [24] or 3 [23] modes. These modes are symmetric (SL) or asymmetric ($S1$, $S2$, and $S3$) related to the type of the compound nucleus and its excitation energy.

In the Gorodisskiy's original approach that has developed for neutron-induced fission, two main parts are considered to generate the mass distribution of fission fragments. The yield of fragment with mass number higher than the half of compound nucleus is indicated by Y_H, and its conjugate with the mass number lower than the half of compound nucleus is indicated with Y_L. These modes are presented as an exponential function with a small deviation from Gaussian shape. Therefore, it is convenient to use the Charlier's distribution [22, 25, 26] to construct the fission fragment mass yield

$$f(u) = 1 - \gamma_1 \left(1/2u - 1/6u^3\right) + \gamma_2 \left(1/24u^4 - 1/4u^2 + 1/8\right), \quad (2)$$

where $u = \frac{(M - <M>)}{\sigma}$ and coefficients γ_1 and γ_2 are, respectively, called dissymmetry and excess and are given by

$$\gamma_1 = \frac{<(M - <M>)^3>}{\sigma^3}$$
$$\gamma_2 = \frac{<(M - <M>)^4>}{\sigma^4} - 3. \quad (3)$$

When $\gamma_1 = \gamma_2 = 0$, the value of Charlier's distribution is equal to one. Values of these parameters for different actinides with their given atomic number are presented in Table 1 [22].

In the original approach of Gorodisskiy, the yield of heavy fragment is defined by the following relation

$$Y_H = \frac{1}{\sqrt{2\pi}} \left(\frac{Y_s \, e^{-1/2 u_s^2}}{\sigma_s} + \frac{Y_a \, e^{-1/2 u_a^2} f(u)}{\sigma_a} \right), \quad (4)$$

where Y_s and Y_a, respectively, correspond to the relative contributions of the symmetric and asymmetric modes of fission in the fragments yield, respectively. Parameters γ_1 and γ_2 are adjusted with the experimental data for each compound nucleus formed after absorbtion of photon [22]. Also, u_a, u_s, σ_a, and σ_s are defined as follows:

$$\sigma_a = \frac{\left(A_{cn} - \upsilon_{pre}\right)\left(Z_{cn} - 73\right)\left(0.074 + 0.0296\sqrt[4]{E}\right)}{Z_{cn}}, \quad (5)$$

$$\sigma_s = \frac{0.031\left(A_{cn} - \upsilon_{pre}\right)\sqrt[4]{E}}{\sqrt{90.54 - 1.9\frac{Z_{cn}^2}{A_{cn} - \upsilon_{pre}}}} + 9.64, \quad (6)$$

$$u_s = \frac{A - \left(A_{cn} - \upsilon_{pre}\right)/2}{\sigma_s} \quad (7)$$

and

$$u_a = \frac{A - \alpha}{\sigma_a}. \quad (8)$$

where $\alpha = 54\frac{A_{cn} - \upsilon_{pre}}{Z_{cn}}$ for $Z_{cn} = 90$–91 and $\alpha = 28.6\frac{A_{cn} - \upsilon_{pre}}{Z_{cn}} + 0.708 Z_{cn}$ for $Z_{cn} \geq 92$. A_{cn} and Z_{cn} are, respectively, the mass and charge numbers of compound nucleus. υ_{pre} is the average pre-scission neutron multiplicity and E is the gamma-rays energy. Also, A is the mass number of the nascent fragment. In order to calculate the values of Y_a and

Table 1 Values of γ_1 and γ_2 for various actinides with definite Z_{cn}

Z_{cn}	90	91	92	93	94	95
γ_1	0	− 0.08	0.36	0.23	0.3	0.38
γ_2	− 0.36	− 0.07	− 0.34	− 0.27	− 0.3	− 0.34

Y_s in Eq. (3), the ratio $\frac{Y_a}{Y_s}$ is obtained through the fitting method with the experimental data as follows:

$$\frac{Y_a}{Y_s} = 1.244\left(1 - e^{-0.0027(|E-5.7|)^{3/2}}\right)\left(\sqrt[4]{E} + 100\left(\frac{Z_{cn}}{A_{cn}} - 0.4\right)\right), \quad (9)$$

and the values of Y_a and Y_s are obtained by replacing this ratio in the following equations

$$Y_a = 200\left(\left|\frac{Y_a}{Y_s}\right| + 2\right)^{-1} \quad (10)$$

and

$$Y_s = 200 - 2Y_a. \quad (11)$$

In a similar way, the yield of light conjugate fragment(Y_L)is also obtained by replacing M_L with $A_{cn} - A$. Finally, the fission fragment mass yield is evaluated using the following equation

$$Y = Y_H + Y_L. \quad (12)$$

Equation (9) is revised by considering two adjustable parameters β and δ, instead of their fixed values in the original formalism of Gorodisskiy as,

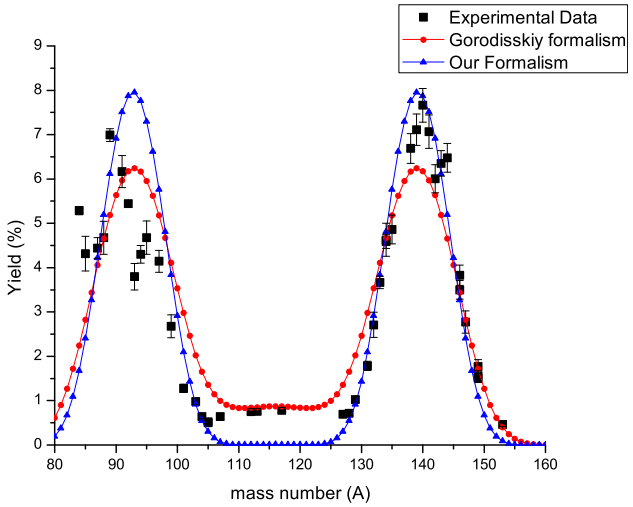

Fig. 1 (Color online) Photofission fragment mass yield at 16 MeV for ^{232}Th: comparison between the experimental data [28], the results of Gorodisskiy's formalism and the results of present study

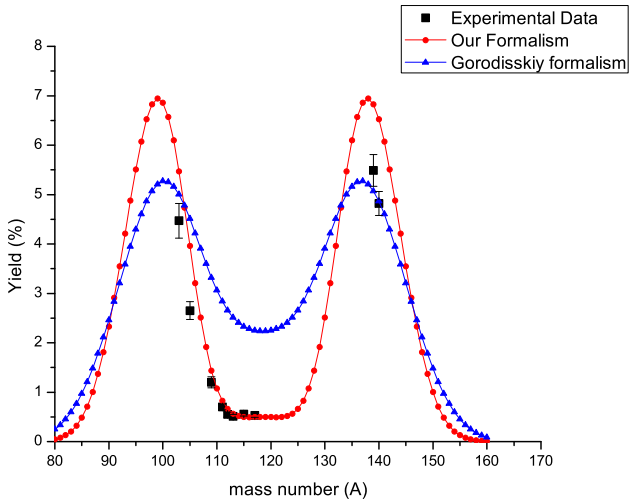

Fig. 3 (Color online) Photofission fragment mass yield at 24 MeV for ^{237}Np: comparison between the experimental data [34], the results of Gorodisskiy's formalism and the results of present study

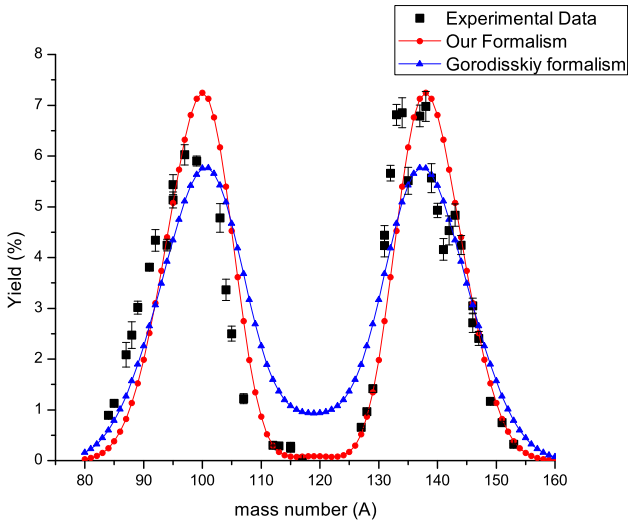

Fig. 2 (Color online) Photofission fragment mass yield at 17.2 MeV for ^{238}U: comparison between the experimental data [31], the results of Gorodisskiy's formalism and the results of present study

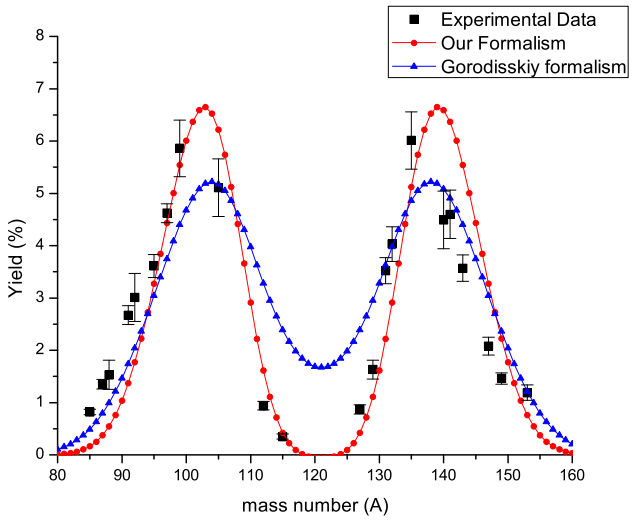

Fig. 4 (Color online) Photofission fragment mass yield at 20 MeV for ^{242}Pu: comparison between the experimental data [38], the results of Gorodisskiy's formalism and the results of present study

$$\frac{Y_a}{Y_s} = 1.244\left(1 - e^{-0.0027(|E-5.7|)^{\delta}}\right)\left(\sqrt[\beta]{E} + 100\left(\frac{Z_{cn}}{A_{cn}} - 0.4\right)\right). \quad (13)$$

The parameters β and δ are obtained using the fitting method with experimental data. The developed approach is used to calculate the photofission fragment mass yield of various actinides at different energies.

3 Results and discussion

The revised formalism presented in this paper is applied to calculate the fragments mass distribution in photofission reactions of ^{232}Th at 16 MeV, ^{238}U at 17.2 MeV, ^{237}Np at 24 MeV, and ^{242}Pu at 20 MeV and compared with the results of Gorodisskiy's formalism as well as the experimental data in Figs. 1, 2, 3 and 4. As it is clear from Figs. 1, 2, 3 and 4, the fission fragment mass yields of the present formalism are in better agreement with experimental data than the Gorodisskiy's original formalism. However, there is some

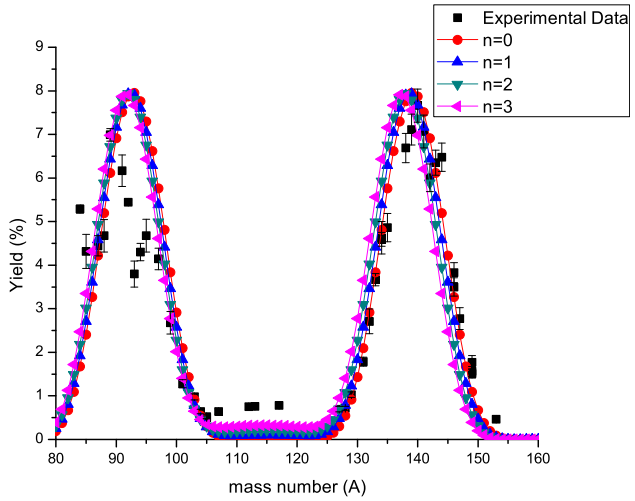

Fig. 5 (Color online) Photofission fragments mass yield at 14 MeV for ^{232}Th: comparison between the experimental data [28] and the results of present study by considering 1, 2, and 3 neutrons emitted prior to fission

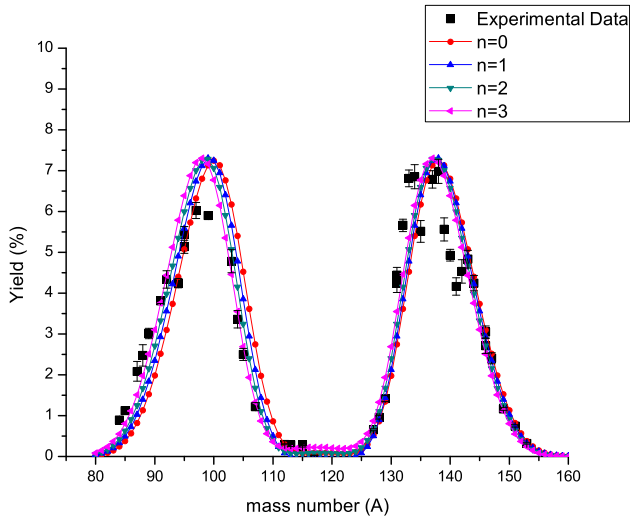

Fig. 6 (Color online) Photofission fragment mass yield at 17.2 MeV for ^{238}U: comparison between the experimental data [31] and the results of present study by considering 1, 2, and 3 neutrons emitted prior to fission

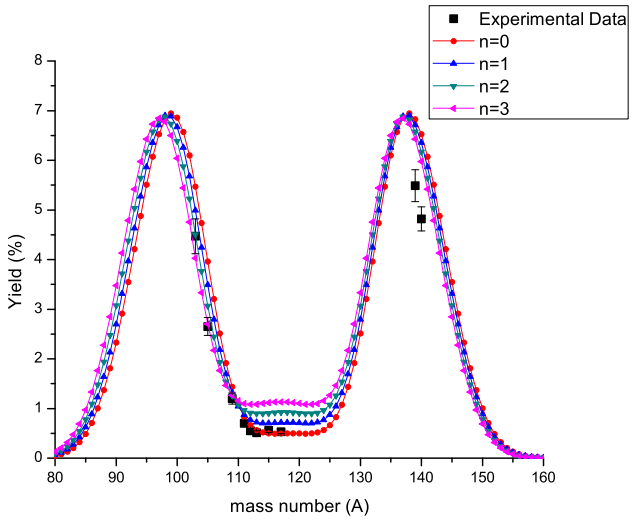

Fig. 7 (Color online) Photofission fragment mass yield at 24 MeV for ^{237}Np: comparison between the experimental data [34] and the results of present study by considering 1, 2, and 3 neutrons emitted prior to fission

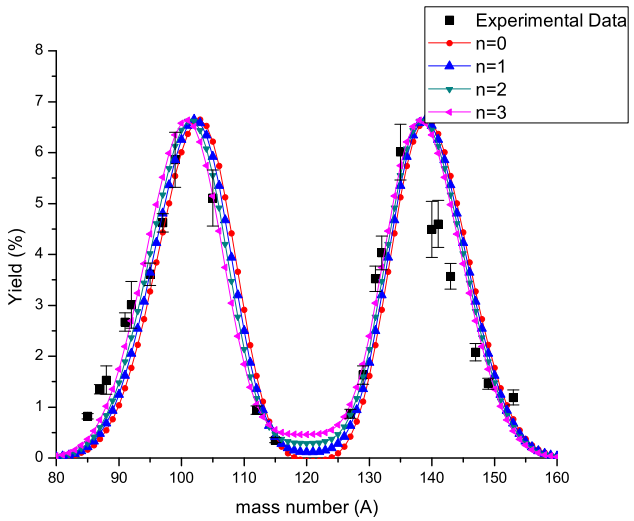

Fig. 8 (Color online) Photofission fragment mass yield at 20 MeV for ^{242}Pu: comparison between the experimental data [38] and the results of present study by considering 1, 2 and 3 neutrons emitted prior to fission

inconsistency between the calculated results and the experimental data especially in the most probable fragmentation, around the maximum of fragment yields.

In Figs. 5, 6, 7 and 8, the calculated results of fission fragment yields considering 1, 2, 3 and 4 pre-scission neutron multiplicity prior to fission are compared with the experimental data for photofission reactions of ^{232}Th at 14 MeV, ^{238}U at 17.2 MeV, ^{237}Np at 24 MeV, and ^{242}Pu at 20 MeV. These figures indicate that the emission of neutrons prior to fission does not considerably affect the photofission fragment mass yield. This is one of the Gorodisskiy formalisms drawbacks that is not able to properly indicate the role played by neutron emission in photofission. In order to calculate the fission fragment mass yield as a function of fragment atomic number, (Z), following the semiempirical formula between the fragment mass, (A) and its atomic number, (Z) is employed

$$A = \frac{A_{cn}}{Z_{cn}}(Z - 2.5). \quad (14)$$

The fragment mass yield of photofission for ^{238}U at 11.39 MeV and 13.39 MeV is calculated and indicated as a function of fragments atomic number in Fig. 9a and b, respectively. This figure shows that the fragment mass yield of the present formalism for ^{238}U is better fitted with the experimental data [31].

Generally, high-energy photons used in photofission studies are generated through the Bremsstrahlung effect of accelerated electron beam crossing dense conversion targets. The maximum electron energy is called the end-point energy and the average compound nucleus excitation energy corresponding to such end-point energy is an important factor to reproduce the experimental data. Naik et al. [30] determined the photofission fragment mass yield for the ^{240}Pu compound nucleus at 10 MeV photon end-point energy, which is equivalent to the average excitation energy equal to 7.61 MeV. In Fig. 10, the calculated results of fragment mass yield using the present formalism are compared with the experimental data. As it is clear from this figure, by considering the end-point energy instead of average excitation energy, the calculated fragment mass yield is better fitted with the experimental data.

The average mass of the light ($\langle A_L \rangle$) and heavy ($\langle A_H \rangle$) photofission fragments for ^{240}Pu and ^{232}Th actinides are also obtained using the following equation

$$\langle A_L \rangle = \frac{\sum(A \times Y_L)}{\sum Y_L}, \langle A_H \rangle = \frac{\sum(A \times Y_H)}{\sum Y_H}, \quad (15)$$

and the calculated results are compared, respectively, with the experimental data of Thierens et al. [27] and Naik et al.

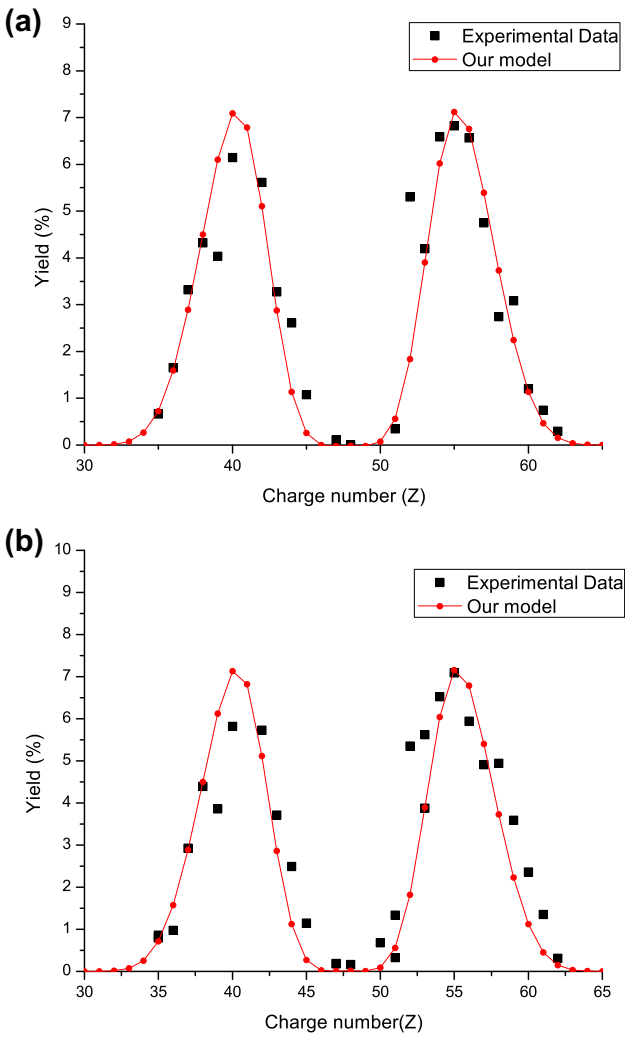

Fig. 9 (Color online) Photofission fragment mass yield at 11.39 MeV (Figure 9a) and 13.39 MeV (Fig. 9b) for ^{238}U: comparison between the experimental data [31] and the results of present study

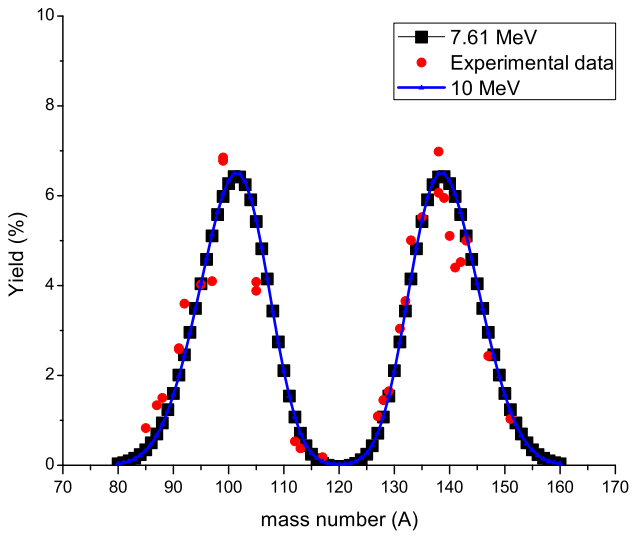

Fig. 10 (Color online) Photofission fragment mass yield at 10 MeV and 7.61 MeV for ^{240}Pu: comparison between the experimental data [30] and the results of present study

Table 2 Average mass of the light and heavy photofission fragments for ^{240}Pu at 30 MeV and ^{232}Th at 80 MeV photon energies are compared with the experimental data

	Our formalism	Thierens [27]	Our formalism	Naik [28]
	^{240}Pu (30 MeV)		^{232}Th (80 MeV)	
$\langle A_L \rangle$	100.57	100.29	92.93	91.74
$\langle A_H \rangle$	139.42	139.71	139.14	136.75

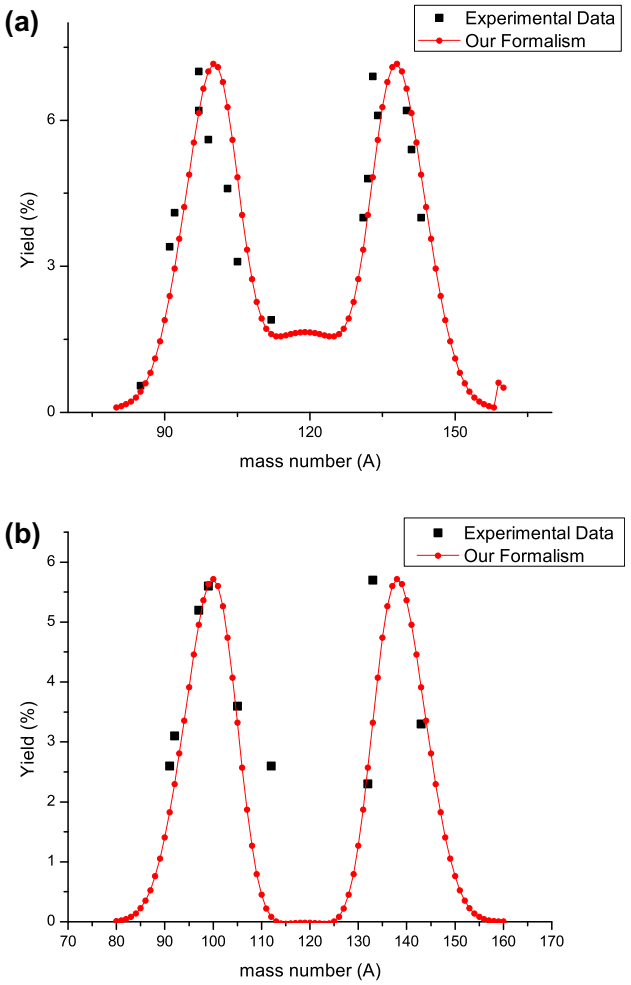

Fig. 11 (Color online) Photofission fragment mass yield at two different high energies, 300 MeV (Fig. 11a) and 500 MeV (Fig. 11b), for ^{238}U: comparison between the experimental data [29] and the results of present formalism

[31] in Table 2. As it can be seen from Table 2, there is a fair agreement between the results of our formalism and the experimental data for ^{240}Pu isotope. A small inconsistency between the results of present formalism and the experimental data [28] for ^{232}Th isotope is produced due to neutron emission through the fission process at high excitation energies. Photofission fragment mass yields for the ^{238}U

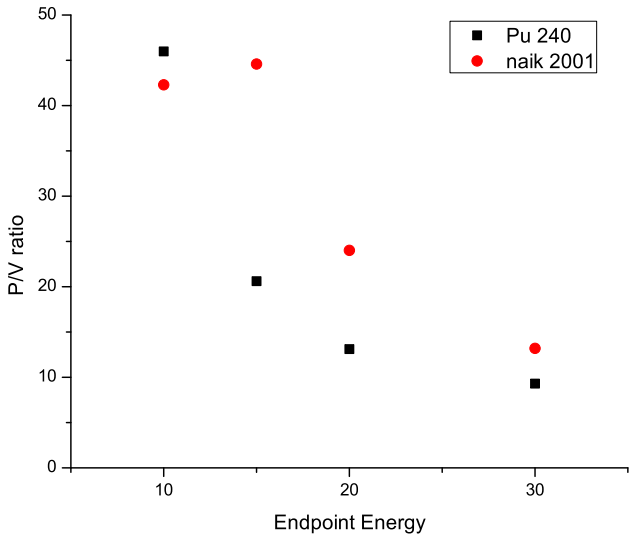

Fig. 12 (Color online) Peak-to-valley ratio as a function of the photon end-point energies (10 → 30 MeV) for ^{240}Pu : comparison between the experimental data [30] and the results of present formalism

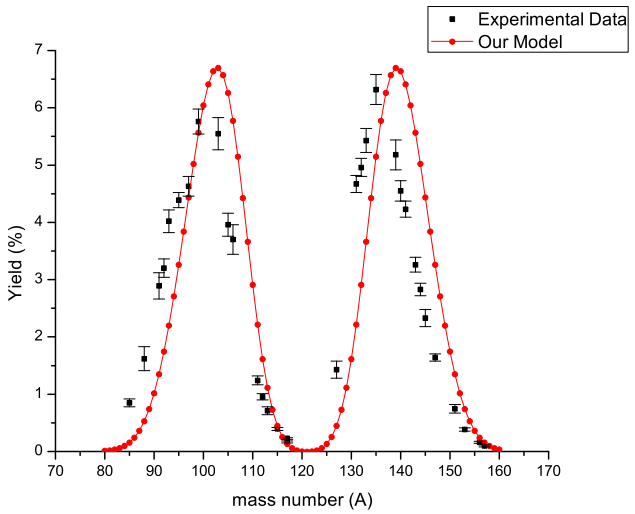

Fig. 13 (Color online) Photofission fragment mass yield at 25 MeV for ^{239}Pu: comparison between the experimental data [36] and the results of present formalism

isotope at 300 and 500 MeV are presented in Fig. 11a and b. It is clear from these figures that the calculated results of the present formalism are in good agreement with the experimental data [29]. It should be noted that the original approach of Gorodisskiy was not successful in reproducing the experimental data of high energy incident photons.

The peak-to-valley ratio of fission fragment yield for the ^{240}Pu compound nucleus is calculated and compared with the experimental data of Naik [30, 32] in Fig. 12. It is clearly indicated in this figure that the peak-to-valley ratio

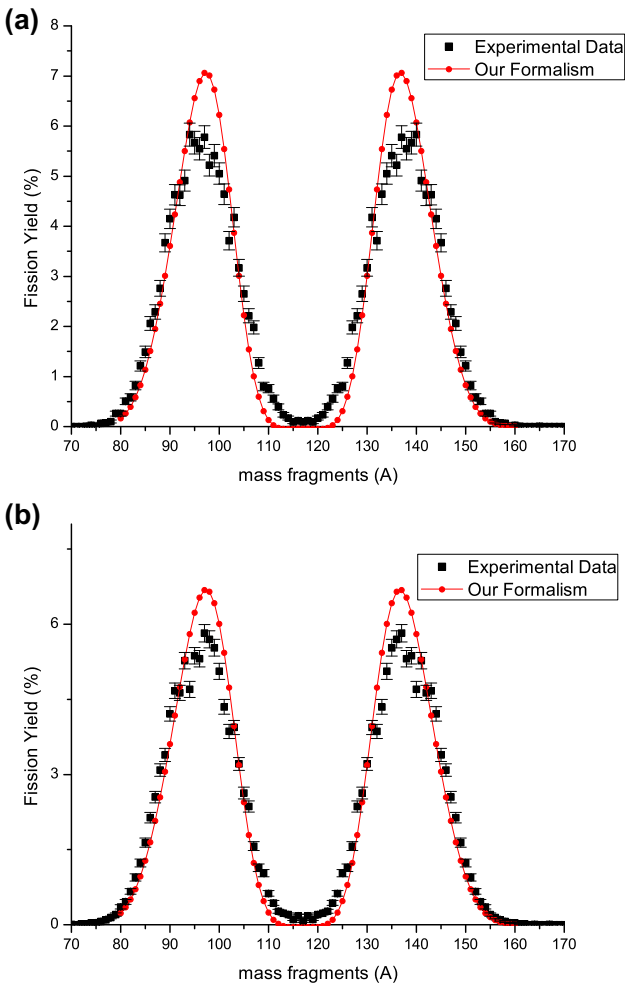

Fig. 14 (Color online) Photofission fragment mass yield at 5.77 MeV (Fig. 13a) and 6.11 MeV (Fig. 13b) for ^{234}U: comparison between the experimental data [39] and the results of present formalism

decreases as the Bremsstrahlung end-point photon energy grows.

The photofission fragment mass yields for the ^{239}Pu isotope at 25 MeV incident photon energy and ^{234}U isotope at 5.77 and 6.11 MeV energies are compared with the experimental data in Figs. 13 and 14. These figures indicate satisfactory agreement between the calculated results of present study and the experimental data except around maximum of the fragment mass yields where the results of the present formalism do not match with the experimental data properly.

4 Conclusion

A phenomenological formula with some adjustable parameters is developed to calculate fission fragment mass yield for ^{232}Th, ^{234,238}U, ^{237}Np, and ^{239,240,242}Pu actinides at various energies. Calculated results are compared with the results of Gorodisskiy's formalism as well as the experimental data. Satisfactory agreement has been achieved between the results of the present formalism and the experimental data especially at low and intermediate photon energies. In this research, the role played by neutron emission prior to fission has also been investigated. It has been stated earlier that the present approach is not able to consider the effect of neutron multiplicity in photofission. The peak-to-valley ratio for photofission of the ^{240}Pu isotope is also obtained and indicated in Fig. 12. Figure 12 shows that the values of peak-to-valley ratio is decreased with the increase in the Bremsstrahlung end-point energies. Generally, it has been shown that the calculated results of the present study are in good agreement with the experimental data as compared with the data reported in Ref. [30].

The average mass of light ($\langle A_L \rangle$) and heavy ($\langle A_H \rangle$) fragments for ^{232}Th and ^{240}Pu actinides are obtained and compared with the experimental data [27, 28]. Good agreement between the results of present approach with the experimental data has also been achieved.

References

1. W. Haxby, W. Shoupp, W. Stephens, Photo-fission of uranium and thorium. Phys. Rev. **59**, 57 (1941). https://doi.org/10.1103/PhysRev.59.57
2. C. Romano, Y. Danon, R. Block, J. Thompson, E. Blain, E. Bond, Fission fragment mass and energy distributions as a function of incident neutron energy measured in a lead slowing-down spectrometer. Phys. Rev. C **81**, 014607 (2010). https://doi.org/10.1103/PhysRevC.81.014607
3. D.M. Gorodisskiy, S.I. Mulgin, A.Y. Rusanov and S.V. Zhdanov, Isotopic invariance of fission fragment charge distributions for actinide nuclei at excitation energies above 10 MeV. Phys. At. Nucl. **66**, 1190 (2003). https://doi.org/10.1134/1.1586436
4. D.M. Gorodisskiy, S.I. Mulgin, V.N. Okolovich, A.Y. Rusanov, S.V. Zhdanov, Isotopic and isotonic effects in fission-fragment mass yields of actinide nuclei. Phys. Lett. B **548**, 45 (2002). https://doi.org/10.1016/S0370-2693(02)02838-1
5. W. Fu Cheng, H. Ji-Min, A study of the multimode fission model. J. Phys. G Nucl. Part. Phys. **15**, 829 (1989). https://doi.org/10.1088/0954-3899/15/6/013
6. P. Moller, J. Randrup, Calculated fission-fragment yield systematics in the region $74 \leq Z \leq 94$ and $90 \leq N \leq 150$. Phys. Rev. C **91**, 044316 (2015). https://doi.org/10.1103/PhysRevC.91.044316
7. M.R. Pahlavani, D. Naderi, Study of fusion cross-section in heavy-ion fusion-fission reactions at around fusion barrier energies using the Langevin dynamical approach. Eur. Phys. J. A **48**, 129 (2012). https://doi.org/10.1140/epja/i2012-12129-y
8. B.D. Wilkins, E.P. Steinberg, Semi-empirical interpretation of nuclear fission based on deformed-shell effects. Phys. Lett. B **42**, 141 (1972). https://doi.org/10.1016/0370-2693(72)90046-9
9. B.D. Wilkins, E.P. Steinberg, R.R. Chasman, Scission-point model of nuclear fission based on deformed-shell effects. Phys. Rev. C **14**, 1832 (1976). https://doi.org/10.1103/PhysRevC.14.1832

10. J. Moreau, K. Heyde, M. Waroquier, Nuclear temperature effects in the scission-point model of nuclear fission. Phys. Rev. C **28**, 1640 (1983). https://doi.org/10.1103/PhysRevC.28.1640
11. A.R. DeL Musgrove, J.L. Cook, G.D. Trimble, in *Proceedings Fifteenth Annual ACM, Bologna, V. II in IAEA-169*, vol 163 (1974)
12. A.C. Wahl, Nuclear-charge distribution and delayed-neutron yields for thermal-neutron-induced fission of ^{235}U, ^{233}U, and ^{239}Pu and for spontaneous fission of ^{252}Cf. At. Data Nucl. Data Tables **39**, 1 (1988). https://doi.org/10.1016/0092-640X(88)90016-2
13. J. Katakura, in *Report JAERI-Research* (2003–2004)
14. R.W. Mills, *Fission Product Yield Evaluation*, Ph.D thesis (School of Physics and Space Research, University of Birmingham, 1995)
15. K.-H. Schmidt, B. Jurado, C. Amouroux, C. Schmitt, General description of fission observables: GEF model code. Nucl. Data Sheets **131**, 107 (2016). https://doi.org/10.1016/j.nds.2015.12.009
16. M.R. Pahlavani, S.M. Mirfathi, Neutron-induced fission of even- and odd-mass plutonium isotopes within a four-dimensional Langevin framework. Phys. Rev. C **96**, 014606 (2017). https://doi.org/10.1103/PhysRevC.96.014606
17. M.R. Pahlavani, S.M. Mirfathi, Dynamical simulation of neutron-induced fission of uranium isotopes using four-dimensional Langevin equations. Phys. Rev. C **93**, 044617 (2016). https://doi.org/10.1103/PhysRevC.93.044617
18. M.R. Pahlavani, S.M. Mirfathi, Dynamics of neutron-induced fission of ^{235}U using four-dimensional Langevin equations. Phys. Rev. C **92**, 024622 (2015). https://doi.org/10.1103/PhysRevC.92.024622
19. M.R. Pahlavani, S.M. Mirfathi, Dynamical simulation of neutron-induced fission of uranium isotopes using four-dimensional Langevin equations. Eur. Phys. J. A **52**, 95 (2016). https://doi.org/10.1103/PhysRevC.93.044617
20. J. Randrup, P. Moller, Brownian shape motion on five-dimensional potential-energy surfaces: nuclear fission-fragment mass distributions. Phys. Rev. Lett. **106**, 132503 (2011). https://doi.org/10.1103/PhysRevLett.106.132503
21. J. Randrup, P. Moller, A.J. Sierk, Calculated fission yields of neutron-deficient mercury isotopes. Phys. Rev. C **85**, 024306 (2012). https://doi.org/10.1103/PhysRevC.85.024306
22. D.M. Gorodisskiy, K.V. Kovalchuk, S.I. Mulgin, Systematics of fragment mass yields from fission of actinide nuclei induced by the 5–200 MeV protons and neutrons. Ann. Nucl. Energy **35**, 238 (2008). https://doi.org/10.1016/j.anucene.2007.06.002
23. U. Brosa, S. Grossmann, A. Mller, Nuclear scission. Phys. Rep. **197**, 167 (1990). https://doi.org/10.1016/0370-1573(90)90114-H
24. D.M. Gorodisskiy, S.I. Mulgin, A.Y. Rusanov et al., The new-revealed regularities of fragments mass yield from the proton induced fission of actinide nuclei, in *Proceedings of the 5th International Conference on Dynamical Aspects of Nuclear Fission* pp. 287. https://doi.org/10.1142/9789812776723-0023 (2002)
25. S.I. Mulgin, V.N. Okolovich, S.V. Zhdanov, Observation of new channel in the proton-induced low-energy fission of nuclei from ^{233}Pa to ^{245}Bk. Phys. Lett. B **462**, 29 (1999). https://doi.org/10.1016/S0370-2693(99)00859-X
26. I.V. Pokrovsky, M.G. Itkis, J.M. Itkis, Fission modes in the reaction ^{208}Pb(^{18}O, f). Phys. Rev. C **62**, 014615 (2000). https://doi.org/10.1103/PhysRevC.62.014615
27. H. Thierens, A. De, E.J. Clercq, Kinetic energy and fragment mass distributions for ^{240}Pu(s.f.), ^{239}Pu(n_{th}, f), and ^{240}Pu(γ, f). Phys. Rev. C **23**, 2104 (1981). https://doi.org/10.1103/PhysRevC.23.2104
28. H. Naik, G.N. Kim, R. Schwengner, Fission product yield distribution in the 12, 14, and 16 MeV bremsstrahlung-induced fission of ^{232}Th. Eur. Phys. J. A **51**, 150 (2015). https://doi.org/10.1140/epja/i2015-15150-8
29. B. Schroder, G. Nydahl, B. Forkman, High-energy photofission in ^{238}U, ^{232}Th and ^{209}Bi. Nucl. Phys. A **143**, 449 (1970). https://doi.org/10.1016/0375-9474(70)90541-5
30. H. Naik, V.T. Nimje, D. Raj, Mass distribution in the bremsstrahlung-induced fission of ^{232}Th, ^{238}U and ^{240}Pu. Nucl. Phys. A **853**, 1 (2011). https://doi.org/10.1016/j.nuclphysa.2011.01.009
31. H. Naik, F. Carrel, G.N. Kim et al., Mass yield distributions of fission products from photo-fission of ^{238}U induced by 11.5 $\rightarrow$ 17.3 MeV bremsstrahlung. Eur. Phys. J. A Hadrons Nucl. **49**, 94 (2013). https://doi.org/10.1140/epja/i2013-13094-7
32. S.S. Belyshev, B.S. Ishkhanov, A.A. Kuznetsov et al., Mass yield distributions and fission modes in photofission of ^{238}U below 20 MeV. Phys. Rev. C **91**, 034603 (2015). https://doi.org/10.1103/PhysRevC.91.034603
33. E. Jacobs, H. Thierens, D. De Frenne et al., Product yields for the photofission of ^{238}U with 12, 15, 20, 30, and 70 MeV bremsstrahlung. Phys. Rev. C **19**, 422 (1979). https://doi.org/10.1103/PhysRevC.19.422
34. M.Y. Kondrat'ko, V.N. Korinets, K.A. Petrzhak, The fragment yields in Np-237 photofission. Sov. At. Energy **35**, 862 (1973). https://doi.org/10.1007/BF01164117
35. H. Thierens, E. Jacobs, P. D'hondt et al., Fragment mass and kinetic energy distributions for ^{242}Pu(sf), ^{241}Pu(n_{th}, f), and ^{242}Pu(γ, f). Phys. Rev. C **29**, 498 (1984). https://doi.org/10.1103/PhysRevC.29.498
36. M.Y. Kondratko, A.V. Mosesov, K.A. Petrzhak, Product yields of photofission of Pu-239. Sov. At. Energy **50**, 41 (1981). https://doi.org/10.1007/BF01141251
37. P. David, J. Debrus, U. Kim, High-energy photofission of gold and uranium. Nucl. Phys. A **197**, 163 (1972). https://doi.org/10.1016/0375-9474(72)90753-1
38. V.D. Bang, Y.S. Zamyatnin, C.D. Tkhien, Yield of Pu-242 photofission fragments. Sov. At. Energy **58**, 320 (1985). https://doi.org/10.1007/BF01207227
39. A. Gk, M. Chernykh, C. Eckardt, Fragment characteristics from fission of ^{238}U and ^{234}U induced by 6.5 to 9.0 MeV bremsstrahlung. Nucl. Phys. A **851**, 1 (2011). https://doi.org/10.1016/j.nuclphysa.2010.12.012